

# ParallelVLM: Lossless Video-LLM Acceleration with Visual Alignment Aware Parallel Speculative Decoding

Quan Kong, Yuhao Shen, Yicheng Ji, Huan Li, Cong Wang  
Zhejiang University, Hangzhou, China

{qkv, riven, jiyicheng.cs, lihuan.cs, cwang85}@zju.edu.cn

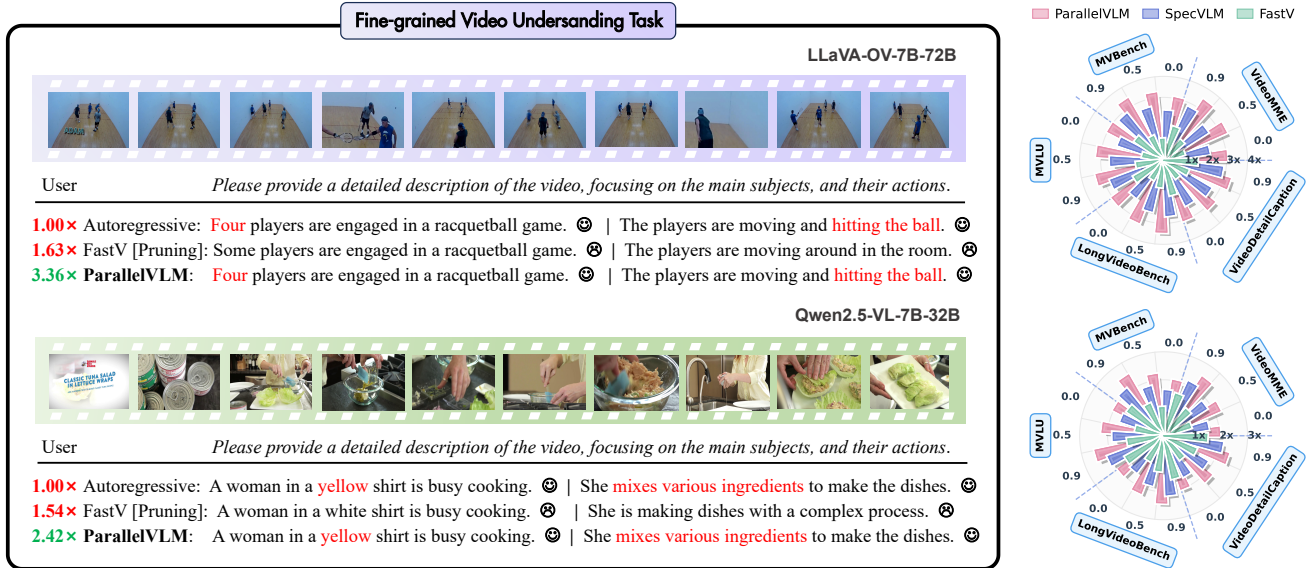


Figure 1. Comparison of ParallelVLM with vanilla autoregressive decoding and visual token pruning. ParallelVLM achieves up to 3.36× acceleration for LLaVA-OV-72B and 2.42× for Qwen2.5-VL-32B across various video understanding benchmarks.

## Abstract

Although current Video-LLMs achieve impressive performance in video understanding tasks, their autoregressive decoding efficiency remains constrained by the massive number of video tokens. Visual token pruning can partially ease this bottleneck, yet existing approaches still suffer from information loss and yield only modest acceleration in decoding. In this paper, we propose ParallelVLM, a training-free draft-then-verify speculative decoding framework that overcomes both mutual waiting and limited speedup-ratio problems between draft and target models in long-video settings. ParallelVLM features two parallelized stages that maximize hardware utilization and incorporate an Unbiased Verifier-Guided Pruning strategy to better align the draft and target models by eliminating the positional bias in attention-guided pruning. Extensive experiments demonstrate that ParallelVLM effectively expands the draft win-

dow by 1.6 ~ 1.8× with high accepted lengths, and accelerates various video understanding benchmarks by 3.36× on LLaVA-Onevision-72B and 2.42× on Qwen2.5-VL-32B compared with vanilla autoregressive decoding.

## 1. Introduction

The advent of Large Language Models (LLMs) has ushered a new era in AI with foundational models like GPT-5, LLaMA, Qwen and Deepseek [1, 9, 40]. This success has quickly catalyzed multimodal research [24, 27, 32, 44], such as Video-LLMs [3, 20, 26], enabling a wide range of new applications like video understanding [12], content auditing [28], and autonomous driving [34].

Despite these advances, the practical deployment of Video-LLMs is hampered by inference latency. State-of-the-art models like LLaVA-OneVision [20] typically encode videos into long sequences of visual tokens, which can easily scale from thousands to millions. Due to the quadratic

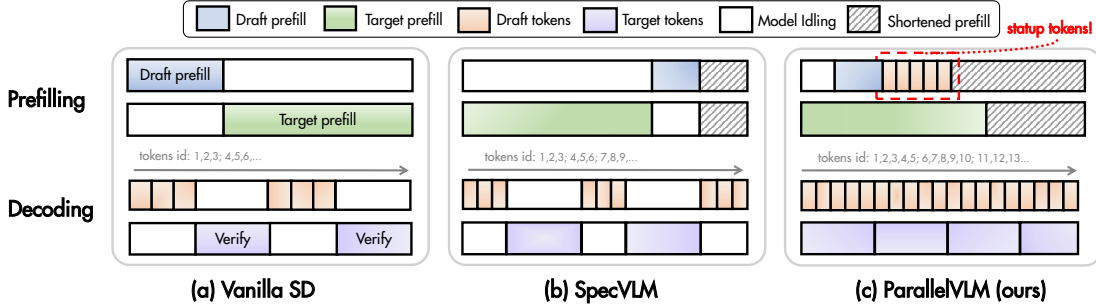


Figure 2. Comparison of different training-free speculative decoding frameworks for Video-LLMs. (a) Vanilla SD: sequential in both prefilling and decoding stages, achieving speedup only with the draft-then-verify design. (b) SpecVLM [18]: inherits vanilla SD and enables faster draft model execution via attention-guided pruning. (c) ParallelVLM: adopts a parallel pipeline to mitigate idling time in vanilla SD, co-designed with UV-Prune strategy to expand the draft window size meanwhile preserving draft/target alignment.

computational cost of self-attention [41], such an explosion in token length creates a crippling performance bottleneck in both prefilling (KV cache computation) and decoding. To address this challenge, numerous efforts have been devoted to designing more effective visual token pruning methods [7, 39, 47, 50]. However, as shown in Fig. 1, since autoregressive access to the full model parameters is still required, they only offer limited acceleration. Even worse, *pruning without validation* induces inevitable distributional shifts that cause measurable performance degradation, particularly in fine-grained video understanding tasks.

To achieve lossless acceleration, *Speculative Decoding* (SD) offers a promising alternative [6, 19, 45] and SpecVLM has pioneered the application of SD to Video-LLMs [18]. As shown in Fig. 2 (a), SD replaces autoregressive decoding with a draft-then-verify paradigm, achieving a theoretical speedup proportional to the speed ratio of the draft/target model pairings. However, when applied to Video-LLMs, existing SD frameworks face two new challenges. (i) **Sequential Execution**: SD enforces strict sequential execution indicated by the idling gaps in Fig. 2 (a/b), which becomes costly with massive visual token prefixes in Video-LLMs. (ii) **Entanglement between Speed Ratio and Model Alignment**: visual tokens often contain substantial redundancy and the draft model can be pruned to improve the draft/target speed ratio. However, draft models with pruned visual tokens often struggle to retain both salient visual details and coherent textual grounding to align with the target model’s distribution. While SpecVLM attempts to guide the draft model pruning with the target’s attention scores [18], it suffers from the “positional bias” problem [11], which in turn hurts model alignment for videos rich in temporal and spatial semantic cues.

To address these challenges, we propose ParallelVLM, a co-design of parallel SD and draft video token pruning. Our framework combines prefilling/decoding parallelism and an Unbiased Verifier-Guided Pruning (UV-Prune) strategy to expand the draft window size without sacrificing alignment. As illustrated in Fig. 2 (c), ParallelVLM entails Parallel Pre-

filling (PP) and Parallel Decoding (PD) stages: 1) in PP, the draft model’s *pruned* prefilling executes concurrently with the target’s *full* prefilling, in which pruning decisions are guided by the vision-text variation signals from the target’s early-layer representations. This mitigates positional bias and hides the draft’s pruning/start-up timing cost under the target’s latency. 2) In PD, draft token generation and target verification proceed in overlapping windows with an optimal window size determined by the enlarged draft/target speed ratio. The draft/target pairings also preserve a high accepted length with the alignment-aware design. Our contributions are summarized as follows:

- ✦ **Systematic Analysis.** We conduct a comprehensive analysis on SD efficiency for Video-LLMs, identifying the sequential execution bottleneck and the coupling relations between draft/target speed ratio and model alignment.
- ✦ **Parallel Acceleration Framework.** We propose ParallelVLM, a *training-free and lossless* architecture that leverages parallelism and unbiased pruning to expand the draft window while maintaining robust acceptance rates.
- ✦ **Significant Speedups.** Extensive experiments on five video understanding benchmarks show ParallelVLM achieves up to  $3.36\times$  and  $2.42\times$  speedups for the LLaVA-OneVision-72B and Qwen2.5-VL-32B respectively.

## 2. Preliminary

### 2.1. Video Large Language Models (Video-LLMs)

A typical Video-LLM consists of: 1) a vision encoder  $E$  that transforms input video frames into a sequence of feature vectors; 2) an adapter  $g_\theta$  that maps these visual features into the language model’s embedding space; and (3) a large language model that processes the combined multimodal input [3, 20]. Formally, a video input is processed into a sequence of visual tokens  $V_{1:m} := [V_1, \dots, V_m]$  and the text is tokenized into  $X_{1:n} := [X_1, \dots, X_n]$ . These sequences are concatenated to form a long, multimodal context prefix  $[V_{1:m}, X_{1:n}]$ , where  $m$  could be much larger than  $n$  for Video-LLM. Denote  $p(\cdot)$  as the model distribution, then the

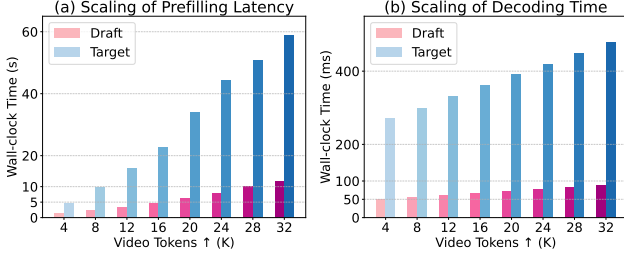


Figure 3. Scaling of (a) Prefilling Latency and (b) Decoding Time with increasing number of video tokens. Experiments are conducted on LLaVA-OV 7B draft model and 72B target model.

subsequent text is generated autoregressively by conditioning on the text prefix of length  $k$  ( $k \geq n$ ):

$$X_{k+1} \sim p(\cdot | V_{1:m}, X_{1:k}). \quad (1)$$

Current visual token pruning methods curtail the video tokens  $V_{1:m}$  before or inner LLM processing, changing the generated token distribution to  $X'_{k+1} \sim p'(\cdot | V'_{1:m}, X_{1:k})$ , inevitably leading to performance degradation.

## 2.2. Speculative Decoding (SD)

SD accelerates autoregressive LLM inference without altering their output distribution [6, 19, 45]. The core of SD operates on a *draft-then-verify principle*: a lightweight *draft model*  $M_q$  generates  $\gamma$  candidate tokens. These tokens are then verified in a single, parallel forward pass by the more powerful target model  $M_p$ . Denote the single forward time of the draft and target model as  $T_q$  and  $T_p$ , respectively, then the speed ratio  $c = T_p/T_q$  normally satisfies  $c \gg 1$ .

The lossless nature of SD is guaranteed by its verification mechanism. With accepted length  $k$ , for each proposed token  $\hat{X}_{k+t}$  in the draft sequence  $\hat{X}_{k+1:k+\gamma}$ , it is accepted with a probability determined by rejection sampling,

$$P(\text{accept}) = \min \left\{ 1, \frac{p(\hat{X}_{k+t} | X_{1:k}, \hat{X}_{k+1:k+t-1})}{q(\hat{X}_{k+t} | X_{1:k}, \hat{X}_{k+1:k+t-1})} \right\},$$

where  $p(\cdot)$  and  $q(\cdot)$  are the probability distributions of the target and draft models. If  $\hat{X}_{k+t}$  is rejected, then a new token is sampled from  $\text{norm}(\max(0, p(X_{k+t}) - q(X_{k+t}))$ .

## 3. Why SD Falls Short for Video-LLMs?

**Challenge 1: Sequential Execution Bottleneck.** In vanilla SD, the draft and target models execute prefilling and decoding sequentially on the entire video token sequence. As shown in Fig. 3, the prefilling latency and decoding time become heavier with the increase of video tokens for both the draft and target models. For example, with 24K video tokens, the target’s prefilling takes 44.23 s, and the draft prefilling adds another 7.92 s. When it turns to decoding, the draft decoding time is  $T_q = 78$  ms and the target decoding

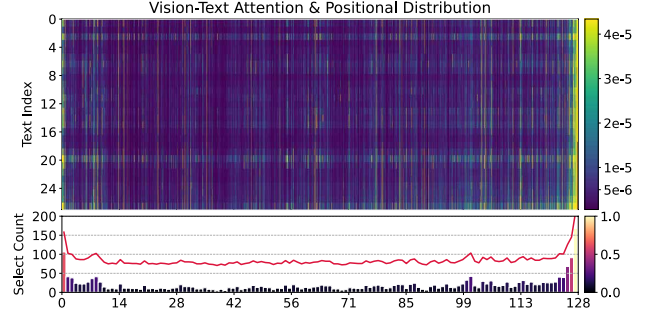


Figure 4. Target model’s attention guidance for draft video token pruning. We observe positional bias on both ends of the video tokens. When retention rate is 10%, frames 1, 125-128 accumulate up to 20.9% of total selected tokens within only 4% position width.

accounts for  $T_p = 420$  ms. With a typical draft window size of  $\gamma = 5$  for the LLaVA-OV-7B/72B combination, the entire cycle takes  $\gamma \cdot T_q + T_p \approx 2T_p$ . This means that the hardware remains idle for almost 20% of the span during prefilling and 50% during decoding due to sequential scheduling. As Video-LLMs require more powerful draft models to understand videos, the sequential waiting becomes even more expensive and persists as a *fixed tax*, whereas the vanilla SD provides no measure to “hide” this overhead.

**Challenge 2: Entanglement between Speed Ratio  $c$  and Model Alignment.** The achievable acceleration in SD is governed by: (i) **speedup ratio**  $c = T_p/T_q$ , which decides how many tokens can be speculated within the target’s verification time; (ii) **model alignment** between draft and target outputs, which controls the acceptance rates. Since video token sequences are known to have high redundancy [4, 7],  $T_q$  can be reduced by pruning the draft visual tokens to improve  $c$ . However, a smaller draft model with pruned tokens often struggles to retain both salient visual details and coherent textual grounding to align with the target model’s full-context distribution. This consequently results in a sharp decrease of the acceptance rates.

To maintain alignment, effective signals from the target model should be utilized to guide the pruning process. SpecVLM [18] leverages attention scores as guidance [18]. Although seemingly intuitive, this approach is undermined by the **positional bias** phenomenon. As shown in Fig. 4, 21% of the attention-guided video tokens are chosen within only 4.0% position width (frames 1, 125-128) simply because they are “attention sinks” [46] or close to the text query [11], not because they are semantically important for visual reasoning and textual grounding. This is particularly problematic for video tasks where temporal coherence and mid-video content matter critically. In addition, attention-guided pruning is incompatible with FlashAttention [8] that adopts block-wise kernels without explicit computation of attention scores. This further prevents them from addressing the I/O bottleneck of Video-LLMs.

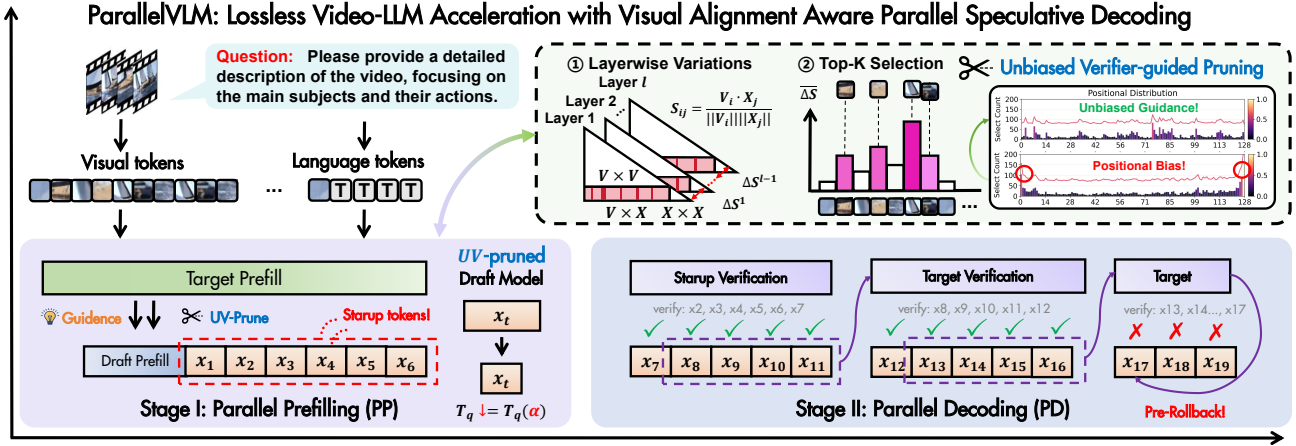


Figure 5. The proposed ParallelVLM consists of Parallel Prefilling (PP), Parallel Decoding (PD) and the Unbiased Verifier-guided Pruning (UV-Prune). (a) During PP stage: draft model prefilling and pruning executes *in parallel* with target model prefilling, where UV-Prune transfers salient alignment semantics from the target model to the draft model without “positional bias”. (b) During PD stage: the reduced draft decoding time  $T_q$  enables an enlarged window size  $\gamma$  *in parallel* with verification, meanwhile maintaining high acceptance rates  $\tau$ .

## 4. Design of ParallelVLM

### 4.1. UV-Prune: Unbiased Verifier-Guided Pruning

Instead of asking “which tokens does the model attend to”, we turn to answer “*which tokens become increasingly aligned with the text query as information flows through the target model layers?*” Tokens whose alignment with the textual query increases across layers are likely carrying task-essential semantics; conversely, tokens whose alignment stays flat or decreases are more likely redundant for the current query. This suggests a new pruning strategy that captures the semantics rather than raw attention scores. Hence, we utilize vision-text similarity variations of the token representations between the shallow layers as the criterion. Specifically, the vision-text similarity is defined as the cosine similarity between the prefilled video tokens  $V_i$  and text tokens  $X_j$  at the pre-defined early layer set  $l \in \{1, \dots, L\}$  from the target model:

$$S_{ij} = \frac{V_i \cdot X_j}{\|V_i\| \|X_j\|}, \quad (2)$$

We then compute the *similarity variation* between consecutive layers and sum over all text tokens,

$$\overline{\Delta S}_i = \sum_{j=1}^n \sum_{l=1}^L (S_{ij}^l - S_{ij}^{l-1}). \quad (3)$$

A large positive  $\overline{\Delta S}_i$  indicates that video token  $V_i$  has gained cross-modal relevance through the network. Given a pruning ratio  $\alpha$  ( $0 < \alpha < 1$ ), we keep the Top- $K$  tokens,

$$V^* = \text{TopK}(\overline{\Delta S}_1, \dots, \overline{\Delta S}_m). \quad (4)$$

As shown in Fig. 5, the similarity variations are signals measured within the target model during its prefilling stage.

Thus, pruning the draft model is directly guided by the target’s own semantics, which provides robust alignment and retains high acceptance rates. Unlike attention scores which bias toward early and query-adjacent tokens, our method reflects a knowledge transfer from the target to the draft model, without being constrained by absolute positions. This enables the natural retention of mid-video frames if there is relevance, preserving both spatial and temporal coherence.

### 4.2. ParallelVLM Pipeline

The ParallelVLM framework executes SD in two fully parallel stages with an overview shown in Fig. 5.

#### Stage I: Parallel Prefilling (PP)

**1 Execution Model.** We launch two independent processes: 1) the target process prefills the full video token sequence  $V_{1:m}$  with the target model  $M_p$ ; 2) the draft process only prefills the pruned video token sequence  $V^*$  with the draft model  $M_q$ . Formally, we have:

$$\text{Parallel} \begin{cases} \text{Draft: } \text{KV}_q \leftarrow M_q(V^*, X_{1:n}) \\ \text{Target: } \text{KV}_p \leftarrow M_p(V_{1:m}, X_{1:n}), \end{cases}$$

in which  $X_{1:n}$  are the text tokens. Since the target prefilling latency is long, all draft-side operations including target-guided pruning, draft prefilling, startup token generation can be completed within this span. This completely hides the draft prefilling time and removes the sequential prefilling bottleneck in vanilla SD.

**2 Verifier-Guided Draft Model Pruning.** Once the target process produce intermediate results of the pre-defined early layers, it broadcasts the target model’s layer-wise token representations to the draft process. The draft process then executes UV-Prune with pruning ratio  $\alpha$  to select the

top  $1 - \alpha$  fraction of video tokens most relevant from the target’s perspective,

$$V^* = \text{UV-Prune}(M_p(V_{1:m}, X_{1:n}), \alpha). \quad (5)$$

③ **Startup Draft Tokens.** The remaining idle time before target prefilling completes is used by the draft process to generate an initial speculative window of  $\gamma$  tokens. These startup tokens are immediately available for verification when Stage I ends, which guarantees that Stage II begins without a warm-up delay.

**Results of Stage I:** After parallel prefilling, (i) the draft model is ready to generate tokens rapidly using the pruned video context. (ii) the target model holds full-context KV caches for lossless verification. (iii) A startup window (e.g.,  $\gamma$  tokens) is already queued for the first verification round.

**Stage II: Parallel Decoding (PD)**

④ **Execution Model.** The draft and target models operate in a coordinated pipeline: in decoding round  $i$  with accepted prefix of length  $k$ , the draft model  $M_q$  generates a window of  $\gamma$  candidate tokens  $\hat{X}_{k+\gamma+1:k+2\gamma}$  from the pruned context  $V^*$ ; simultaneously, the target model  $M_p$  verifies  $\gamma$  tokens drafted in round  $i - 1$  using the full context  $V_{1:m}$ ,

$$\text{Parallel} \begin{cases} \text{Draft}_i : & X_{k+\gamma+t} \sim q(\cdot|V^*, X_{1:k+\gamma+t-1}) \\ \text{Verify}_{i-1} : & X_{k+1:k+\gamma} \sim p(\cdot|V_{1:m}, X_{1:k}) \end{cases}$$

For  $t = 1, \dots, \gamma$ , each candidate token  $\hat{X}_{k+\gamma+t}$  is accepted with rejection sampling illustrated in Sec. 2.2. If a draft token fails verification, sampling resumes from the target distribution for that position. Then the pipeline performs pre-rollback and restart drafting [29].

⑤ **Window Size  $\gamma$  Selection.** The optimal draft window size  $\gamma$  is determined by the pruned speed ratio  $c^*$ :

$$\gamma = c^* = \frac{T_p}{T_q(\alpha)}. \quad (6)$$

$T_q(\alpha)$  is the draft decoding time at pruning ratio  $\alpha$  and  $T_p$  is the target’s verification time with full contexts. As an example, without pruning:  $T_q = 78$  ms,  $T_p = 420$  ms,  $c = T_p/T_q \approx 5$ , so the optimal window size is  $\gamma = 5$ ; with pruning ratio  $\alpha = 0.9$ ,  $T_q = 47$  ms,  $T_p = 420$  ms,  $c = T_p/T_q \approx 9$ , yielding  $\gamma = 9$ , which is  $1.8\times$  larger.

⑥ **Acceptance Rate  $\tau$  Dependency.** The actual speedup depends on the pruning quality through acceptance rate  $\tau$ ,  $\tau = \tau(\mathcal{P}, \alpha)$ . A well-aligned pruning strategy  $\mathcal{P}$  keeps  $\tau$  high even at aggressive pruning ratios ( $\alpha = 0.1$ ).

### 4.3. Theoretical Speedup Analysis

ParallelVLM accelerates Video-LLMs by overlapping the draft and verification stages, and further addressing the visual redundancy of the draft model with the target’s alignment. If the original draft/target speed ratio is  $c$  and the average acceptance rate is  $\tau$ , the theoretical speedup vs. autoregressive decoding is analyzed by the following theorem.

**Theorem 1** (Speedup Ratio of ParallelVLM). *Denote the video token pruning method as  $\mathcal{P}$  and the pruning ratio as  $\alpha \in [0, 1]$ . ParallelVLM overlaps the draft and verification stages, corresponding to an enlarged draft/target speed ratio  $c^*(\alpha) > c$ , and a robust average acceptance rate  $\hat{\tau}(\mathcal{P}, \alpha)$ . For the draft window size of  $\gamma = c^*(\alpha)$ , the speedup ratio of ParallelVLM is,*

$$\mathcal{V}_{\text{ViPSD}} = \frac{\hat{\tau}(\mathcal{P}, \alpha) \cdot \gamma \cdot T_p}{\gamma \cdot T_q(\alpha)} = \hat{\tau}(\mathcal{P}, \alpha) \cdot c^*(\alpha). \quad (7)$$

With the optimal acceptance rate  $\hat{\tau}(\mathcal{P}, \alpha) = 1$ ,  $\mathcal{V}_{\text{ViPSD}} = c^*(\alpha)$  represents  $\frac{c^*(\alpha)}{c} \times$  speedup than Parallel SD [29]. For example, the speedup is  $1.8\times$  for LLaVA-OV-7B/72B and  $1.6\times$  for Qwen2.5-VL-7B/32B. We refer to the Appendix for detailed proofs and a comprehensive comparison with vanilla SD.

## 5. Experiments

### 5.1. Experimental Setting

**Baseline Methods.** For Video-LLMs, autoregressive decoding (AR) is the default decoding setting ( $1.00\times$  baseline). We evaluate the proposed ParallelVLM against a series of *lossless* speculative decoding methods and *lossy* visual token pruning methods. For lossless speculative decoding, we include five methods, which are all plug-and-play with no need of model training.

- Vanilla SD [6]: Standard implementation where a draft model generates  $\gamma$  tokens for target verification.
- OnSD [15]: Light-weight text-only LLM as the draft model for VLM speculative decoding.
- SD-Tree [23]: Speculative decoding with a 5-layer draft tree structure for multi-branch candidate paths.
- SpecVLM [18]: Verifier’s attention-guided draft token pruning for improved Video-LLM speculative decoding.
- STD [49]: KV cache sparsification of the dense target as the draft model for Video-LLM speculative decoding.

For visual token pruning, we collect four dynamic methods that employ the intra-LLM information. We include one-stage importance ranking methods FastV [7], PDrop [47], and two-stage merge-then-sparsify methods SparseVLM [50], DyCoke [39]. Unlike lossless SD methods, pruning is directly performed on the target model.

**Benchmarks and Metrics.** Since ParallelVLM focuses on long-paragraph decoding, we evaluate its performance in video captioning and video description tasks. The benchmarks we use include VideoDetailCaption [31], VideoMME [13], MVBench [21], MVLU [52] and LongVideoBench [43]. For metrics, we assess the acceleration effects with: (i) speedup ratio vs. the autoregressive baseline; (ii) the mean accepted length  $M$  to reflect the speculation accuracy; (iii) token-wise acceptance ratio  $\mathcal{A}$  to

Table 1. Comparison of lossless speculative decoding methods on multiple video understanding tasks. The default window size  $\gamma$  of the baselines is set to 5, except for STD [50] with  $\gamma = 9$ . ParallelVLM achieves adaptive draft length [29], and we dynamically adjust the  $\gamma$  according to the speed ratio  $c = T_p/T_q$  to mitigate mutual waiting. From up to bottom,  $\gamma = \{3, 9, 5, 2, 2\}$  at the pruning ratio  $\alpha = 0.9$ .

Models	Methods	VideoDetailCaption		VideoMME		MVBench		MVLU		LongVideoBench		Avg.
		M	Speedup	M	Speedup	M	Speedup	M	Speedup	M	Speedup	
LLaVA-OV (0.5B & 7B)	Vanilla SD	4.26	1.08×	4.34	1.10×	4.18	1.05×	4.22	1.06×	4.32	1.01×	1.06×
	OnSD	3.73	1.40×	3.67	1.38×	3.78	1.32×	3.56	1.29×	3.76	1.36×	1.35×
	SD-Tree	5.08	1.28×	5.05	1.28×	4.97	1.25×	4.90	1.24×	5.12	1.26×	1.26×
	SpecVLM	4.89	1.83×	4.83	1.82×	4.76	1.77×	4.71	1.76×	4.92	1.86×	1.81×
	ParallelVLM	<b>8.47</b>	<b>2.12×</b>	<b>7.86</b>	<b>2.06×</b>	<b>8.64</b>	<b>2.15×</b>	<b>8.24</b>	<b>2.14×</b>	<b>8.35</b>	<b>2.10×</b>	<b>2.11×</b>
LLaVA-OV (7B & 72B)	Vanilla SD	4.14	1.98×	4.26	2.06×	3.98	1.92×	4.06	2.01×	4.27	2.10×	2.01×
	OnSD	3.67	2.14×	3.65	2.27×	3.48	2.09×	3.69	2.23×	3.74	2.13×	2.17×
	SD-Tree	4.64	2.18×	4.62	2.33×	4.70	2.26×	4.53	2.17×	4.78	2.36×	2.26×
	SpecVLM	4.51	2.76×	4.49	2.80×	4.46	2.68×	4.26	2.62×	4.39	2.82×	2.74×
	ParallelVLM	<b>6.82</b>	<b>3.43×</b>	<b>6.85</b>	<b>3.38×</b>	<b>6.81</b>	<b>3.28×</b>	<b>6.72</b>	<b>3.24×</b>	<b>6.93</b>	<b>3.46×</b>	<b>3.36×</b>
Qwen2.5-VL (7B & 32B)	Vanilla SD	3.37	1.26×	3.44	1.24×	3.38	1.23×	3.21	1.23×	3.47	1.31×	1.25×
	OnSD	2.76	1.38×	2.84	1.32×	2.67	1.27×	2.69	1.34×	2.89	1.36×	1.33×
	SD-Tree	4.21	1.60×	4.32	1.54×	4.17	1.53×	4.09	1.52×	4.23	1.55×	1.55×
	SpecVLM	4.18	2.11×	4.31	2.13×	4.12	2.02×	4.06	2.13×	4.28	2.18×	2.11×
	ParallelVLM	<b>4.23</b>	<b>2.40×</b>	<b>4.37</b>	<b>2.42×</b>	<b>4.24</b>	<b>2.41×</b>	<b>4.15</b>	<b>2.41×</b>	<b>4.43</b>	<b>2.45×</b>	<b>2.42×</b>
LLaVA-OV (7B & 7B)	OnSD	3.60	0.87×	3.64	0.89×	3.57	0.84×	3.28	0.82×	3.12	0.78×	0.84×
	SpecVLM	4.94	1.21×	4.92	1.22×	5.06	1.23×	4.74	1.18×	4.85	1.25×	1.22×
	STD	8.04	1.25×	8.21	1.28×	7.71	1.21×	8.16	1.26×	8.04	1.22×	1.24×
	ParallelVLM	<b>14.8</b>	<b>1.53×</b>	<b>15.6</b>	<b>1.55×</b>	<b>13.2</b>	<b>1.49×</b>	<b>15.7</b>	<b>1.59×</b>	<b>15.0</b>	<b>1.57×</b>	<b>1.55×</b>
Qwen2.5-VL (7B & 7B)	OnSD	3.39	0.82×	2.98	0.78×	3.34	0.83×	3.12	0.74×	3.27	0.80×	0.79×
	SpecVLM	4.80	1.17×	4.91	1.20×	4.93	1.18×	4.98	1.25×	4.85	1.24×	1.21×
	STD	8.03	1.22×	7.89	1.25×	8.11	1.24×	8.02	1.18×	8.23	1.27×	1.23×
	ParallelVLM	<b>14.4</b>	<b>1.52×</b>	<b>14.9</b>	<b>1.53×</b>	<b>14.8</b>	<b>1.47×</b>	<b>14.6</b>	<b>1.50×</b>	<b>15.3</b>	<b>1.53×</b>	<b>1.51×</b>

measure the distribution shifts of lossy visual pruning methods. Due to the lack of long, detailed ground truth description labels, we leverage the target model with full context for evaluation.

**Implementation Details.** Recall that the acceleration of SD mainly depends on the speedup ratio  $c$  and alignment between the draft/target models. For comprehensive evaluation, we evaluate five draft/target pairings across LLaVA-OneVision [20] and Qwen2.5-VL [3], covering  $c$  from 1 – 5 (rounded to nearest integer): (i) LLaVA-OV (0.5B & 7B,  $c = 2$ ), (ii) LLaVA-OV (7B & 72B,  $c = 5$ ), (iii) Qwen2.5-VL (7B & 32B:  $c = 3$ ), (iv) LLaVA-OV (7B & 7B,  $c = 1$ ), (v) Qwen2.5-VL (7B & 7B:  $c = 1$ ). For LLaVA-OneVision, we sample 128 frames for each video with a total of  $196 \times 128 = 25,088$  video tokens; for Qwen2.5-VL, we keep the same number of video tokens accordingly. The max output length is set to  $K = 512$ . All the experiments are conducted with  $8 \times$  L40S GPUs.

## 5.2. Main Results

**Comparison with Lossless SD Methods.** While model combinations with different speed ratios  $c$  greatly influence the overall acceleration, we observe three advantages

of ParallelVLM over the baseline methods. **(i) ParallelVLM achieves significantly better acceleration across the five combinations.** As shown in Tab. 1, ParallelVLM achieves  $2.11\times$ ,  $3.36\times$  and  $2.42\times$  acceleration on average for LLaVA-OV-0.5B/7B, LLaVA-OV-7B/72B, Qwen2.5-VL-7B/32B, respectively. Notably, ParallelVLM surpasses the existing SOTA SpecVLM [18] by  $0.30 \sim 0.64\times$ , mainly attributed to the co-design of the parallel pipeline and UV-Pruning. **(ii) ParallelVLM enables adaptive draft length  $M$  with continuous draft stages.** Unlike vanilla SD framework that requires sequential waiting for draft and verification, ParallelVLM facilitates continuous drafting and simultaneous verification with adaptive draft length [29]. As shown in Tab. 1, ParallelVLM maintains a considerable mean accepted length ( $M$ ) of 8.31, 6.83, 4.28 for the three combinations. The robust acceptance reduces unsuccessful speculation and rollbacks [37], ensuring the overall speedup performance. **(iii) ParallelVLM makes Self-SD more effective in practice.** Self-SD [49] is a special paradigm with perfect alignment traded by a smaller speed ratio  $c$ . While vanilla SD methods wait for the draft model to finish, ParallelVLM verifies candidate tokens while drafting, greatly reducing unnecessary waiting time. As shown in the last two

Table 2. Comparison of lossy visual token pruning methods on multiple video understanding tasks. ParallelVLM achieves a superior speedup ratio losslessly. (The minor drops stem from the inherent uncertainty of LLMs and the precision limits of hardware numerics.)

Methods	VideoDetailCaption		VideoMME		MVBench		MVLU		LongVideoBench		Avg.	
	$\mathcal{A}$	Speedup	$\mathcal{A}$	Speedup	$\mathcal{A}$	Speedup	$\mathcal{A}$	Speedup	$\mathcal{A}$	Speedup	$\mathcal{A}$	Speedup
LLaVA-OV-72B, Average Retention Ratio=10%												
FastV	83.2%	1.60×	85.7%	1.65×	84.1%	1.62×	86.3%	1.66×	83.7%	1.62×	84.6%	1.63×
SparseVLM	88.5%	1.58×	86.2%	1.61×	87.9%	1.59×	85.8%	1.63×	87.1%	1.60×	87.1%	1.60×
P-Drop	86.5%	1.55×	88.9%	1.59×	89.2%	1.57×	87.3%	1.60×	87.1%	1.59×	87.8%	1.58×
DyCoke	92.1%	1.44×	91.5%	1.48×	89.7%	1.46×	90.3%	1.49×	90.9%	1.47×	90.9%	1.47×
ParallelVLM	<b>98.2%</b>	<b>3.43×</b>	<b>99.7%</b>	<b>3.38×</b>	<b>99.5%</b>	<b>3.28×</b>	<b>99.1%</b>	<b>3.24×</b>	<b>98.9%</b>	<b>3.46×</b>	<b>99.1%</b>	<b>3.36×</b>
Qwen2.5-VL-32B, Average Retention Ratio=10%												
FastV	83.7%	1.51×	81.9%	1.53×	80.8%	1.55×	82.6%	1.56×	82.5%	1.55×	82.3%	1.54×
SparseVLM	86.9%	1.48×	84.3%	1.51×	85.7%	1.49×	83.8%	1.52×	86.3%	1.50×	85.4%	1.50×
P-Drop	83.2%	1.49×	85.9%	1.53×	84.1%	1.51×	86.4%	1.52×	84.0%	1.55×	84.7%	1.52×
DyCoke	88.9%	1.42×	86.7%	1.45×	87.3%	1.43×	89.1%	1.46×	85.9%	1.44×	87.6%	1.44×
ParallelVLM	<b>98.8%</b>	<b>2.40×</b>	<b>98.2%</b>	<b>2.42×</b>	<b>98.6%</b>	<b>2.41×</b>	<b>99.2%</b>	<b>2.41×</b>	<b>98.7%</b>	<b>2.45×</b>	<b>98.7%</b>	<b>2.42×</b>

rows in Tab. 1, Self-SD achieves a mean accepted length of  $M > 14$ , with an acceleration of  $1.51 \sim 1.55\times$ , which accounts for  $\sim 0.30\times$  higher speedup than SpecVLM [18] and STD [49] methods.

**Comparison with Lossy Visual Token Pruning Methods.** Compared with vanilla visual token pruning methods [7, 39, 47, 50], ParallelVLM is favorable from the two following aspects. **(i) ParallelVLM has a theoretically lossless guarantee.** As shown in Tab. 2, although FastV [7], SparseVLM [50], P-Drop [47], DyCoke [39] can reduce video tokens without a draft-then-verify framework, they inevitably lead to performance degradation ( $-9.1\% \sim -17.7\%$ ). Therefore, it is questionable for their practical applications, particularly in tasks demanding fine-grained details. In contrast, ParallelVLM presents little information loss with target model verification. **(ii) ParallelVLM offers significantly higher speedup.** While we also observe an alignment-speedup trade-off among visual token pruning methods in Tab. 2, they only provide  $1.44 \sim 1.64\times$  decoding time acceleration. However, ParallelVLM delegates rapid proposals to the 7B draft model, delivering  $3.36\times$  and  $2.42\times$  decoding acceleration for 72B and 32B models, respectively.

### 5.3. Ablation Study

**Effect of Pruning Ratio  $\alpha$ .** Tab. 3 and Fig. 6 confirm that higher draft pruning ratios substantially increase the speed ratio in Eq. (6). As shown in Tab. 3, with the original speedup ratios of  $c = \{5, 3\}$  for LLaVA-OV-7B/72B and Qwen2.5-VL-7B/32B, the speed ratio increases to  $c^* = \{7, 4\}$  at  $\alpha = 0.5$  and  $c^* = \{9, 5\}$  at  $\alpha = 0.9$ , respectively. In ParallelVLM, a larger  $c$  expands the optimal window size  $\gamma$  we can choose within a target model verification time. As shown in Fig. 6, the overall speedup performance increases from  $2.94\times$  to  $3.36\times$  for LLaVA-OV-7B/72B and

Table 3. The speed ratio  $c = T_p/T_q$  with different pruning ratio  $\alpha$ . The forward time is reported in *ms*.

Models	Target $T_p$	Draft $T_q$		
		$\alpha = 0.0$	$\alpha = 0.5$	$\alpha = 0.9$
LLaVA-OV (7B & 72B)	420 ( $\pm 8.64$ )	78.3 ( $\pm 3.46$ ) $c = 5$	57.5 ( $\pm 2.38$ ) $c = 7$	46.6 ( $\pm 1.52$ ) $c = 9$
Qwen2.5-VL (7B & 32B)	203 ( $\pm 6.89$ )	63.7 ( $\pm 2.42$ ) $c = 3$	48.2 ( $\pm 1.66$ ) $c = 4$	39.8 ( $\pm 1.24$ ) $c = 5$

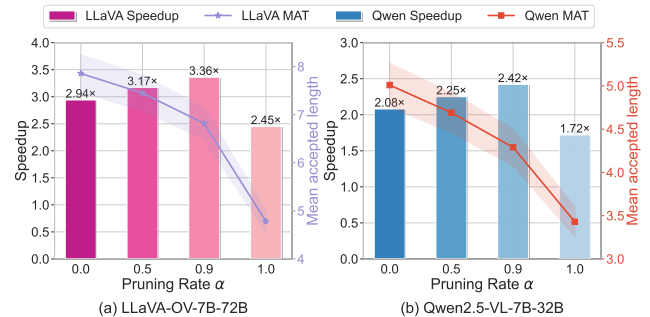


Figure 6. Ablation study of the pruning ratio  $\alpha$ . ParallelVLM strikes a trade-off between speedup and acceptance at  $\alpha = 0.9$ .

from  $2.08\times$  to  $2.42\times$  when  $\alpha$  increases from 0.0 to 0.9. The slight drop in  $M$  at high  $\alpha$  could be offset by the gains of larger  $\gamma$ . However, extreme pruning ( $\alpha = 1.0$ ) breaks alignment and confirms the need for a balanced setting. We observe that  $\alpha = 0.9$  strikes a reasonable balance between the expanded window size and model alignment.

**Impact of Unbiased Verifier-Guided Pruning.** As shown in Fig. 7 (a), UV-Prune effectively mitigates the positional bias of attention-guided pruning meanwhile selectively focusing on different visual cues across frames. In Fig. 7 (b), we further evaluate the alignment of different pruning methods and report the mean accepted length  $M$  when  $\alpha = 0.9$ .

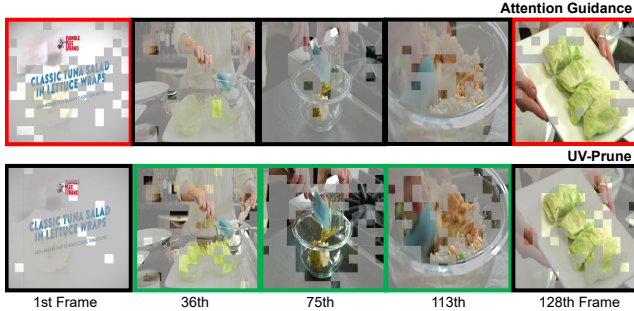


Figure 7. Ablation Study of UV-Prune. (a) Visualizations of selected tokens across frames. (b) Impact of UV-Prune’s verifier-guidance and similarity-variation. With the joint effort of the two components, ParallelVLM achieves robust acceptance, exceeding existing baselines.

For comparison, although SpecVLM [18] leverages the target model’s attention scores for guidance, it provides only partial accurate alignment due to positional bias and  $M$  drops by 0.2. For other methods without verifier guidance, the accept length drops more sharply by  $0.3 \sim 0.5$ . In contrast, UV-Prune consistently achieves a higher accepted length.

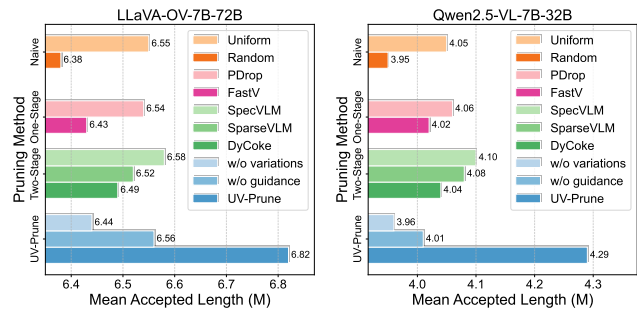
**FlashAttention Compatibility.** Because UV-Prune does not rely on explicit attention-score computation, it is fully compatible with FlashAttention [8]. Tab. 4 demonstrates increasing benefits with longer sequence lengths. At 24K sequence length, FlashAttention adds  $1.35\times$  extra speedup on top of ParallelVLM and at 32K, the gain further reaches to  $1.41\times$ . With an increasing demand for long video understanding tasks, the compatibility with efficient attention operators is increasingly important in the future.

Table 4. Integration of flash attention at different sequence lengths. The forward time is reported for LLaVA-OV-72B in *ms*.

	Sequence Length			
	8K	16K	24K	32K
w/o flash.	302 ( $\pm 6.15$ )	361 ( $\pm 7.06$ )	420 ( $\pm 8.32$ )	479 ( $\pm 9.14$ )
w/ flash.	248 ( $\pm 4.42$ )	280 ( $\pm 4.67$ )	311 ( $\pm 5.21$ )	340 ( $\pm 6.08$ )
Speedup	$1.22\times$	$1.29\times$	$1.35\times$	$1.41\times$

## 6. Related Work

**Visual Token Pruning for VLMs.** A plethora of works have identified substantial redundancy in visual tokens and proposed pruning strategies to speed up VLMs. Existing approaches can generally be grouped into pre-LLM [2, 17, 30, 33, 36, 38, 42, 48] and intra-LLM pruning [7, 39, 47, 50]. The pre-LLM methods (e.g. PruMerge [33] and FastVID [36]) remove redundant tokens at the vision encoder stage before they are passed to the language model, leveraging fixed similarity or clustering criteria. Intra-LLM methods (e.g. FastV [7], SparseVLM [50], PDrop [47], DyCoke [39]) dynamically prune or sparsify the KV cache during the LLM’s forward computation. Although visual token pruning methods reduce token load in long-video scenarios,



they offer limited acceleration and cause inevitable distributional shifts that lead to performance degradation.

**Speculative Decoding for LLMs and VLMs.** SD utilizes a lightweight draft model to draft candidate tokens and verify them simultaneously [19, 45], thereby reducing the autoregressive latency of the target model. It can be categorized into draft model training-based [5, 10, 22, 23, 25] and training-free methods [6, 14, 51]. Subsequent works such as PEARL [29], SpecBranch [37] further explore parallel designs. When extended to VLMs, the draft model has been instantiated as a text-only model [15], a distilled model [16], or a lightweight “twig” model [35]. However, naive adaptations to VLM often overlook the fact that draft latency can grow significantly in long-context video understanding, where large amounts of visual tokens must be processed. As a result, current approaches are often ineffective [15] or inefficient [16, 35] for large-scale video inputs.

**Speculative Decoding for Video-LLMs.** The long-context video prefilling contradicts the principle of a lightweight draft model in speculative decoding. To address this challenge, Sparse-to-Dense (STD) [49] introduces a Self-SD framework and utilizes sparse KV cache selection of the dense target model to serve as the draft model. The closest work to ours is SpecVLM [18], which incorporates SD with attention-guided token pruning from the target model. In contrast to standard SD with sequential dependency, we enable complete parallelism while making video token pruning alignment-aware, unbiased and fully compatible with modern hardware optimizations like FlashAttention [8].

## 7. Conclusion

In this paper, we propose ParallelVLM to remove autoregressive decoding bottlenecks in Video-LLMs caused by massive video token inputs. It combines parallel prefilling and parallel decoding with UV-Prune, an attention-free, verifier-guided token reduction method using vision-text similarity variation. By co-designing with parallel SD, our framework improves the speedup ratio while preserving lossless generation, accelerating LLaVA-OV-72B and Qwen2.5-VL-32B by up to  $3.36\times$  and  $2.42\times$ , respectively.

## References

- [1] Josh Achiam, Steven Adler, Sandhini Agarwal, Lama Ahmad, Ilge Akkaya, Florencia Leoni Aleman, Diogo Almeida, Janko Altenschmidt, Sam Altman, Shyamal Anadkat, et al. Gpt-4 technical report. 2023. 1
- [2] Saeed Ranjbar Alvar, Gursimran Singh, Mohammad Akbari, and Yong Zhang. Divprune: Diversity-based visual token pruning for large multimodal models. *2025 IEEE/CVF Conference on Computer Vision and Pattern Recognition (CVPR)*, pages 9392–9401, 2025. 8
- [3] Shuai Bai, Keqin Chen, Xuejing Liu, Jialin Wang, Wenbin Ge, Sibao Song, Kai Dang, Peng Wang, Shijie Wang, Jun Tang, et al. Qwen2.5-vl technical report. *ArXiv*, abs/2502.13923, 2025. 1, 2, 6
- [4] Daniel Bolya, Cheng-Yang Fu, Xiaoliang Dai, Peizhao Zhang, Christoph Feichtenhofer, and Judy Hoffman. Token merging: Your vit but faster. *ArXiv*, abs/2210.09461, 2022. 3
- [5] Tianle Cai, Yuhong Li, Zhengyang Geng, Hongwu Peng, Jason D Lee, Deming Chen, and Tri Dao. Medusa: Simple llm inference acceleration framework with multiple decoding heads. *arXiv preprint arXiv:2401.10774*, 2024. 8, 1
- [6] Charlie Chen, Sebastian Borgeaud, Geoffrey Irving, Jean-Baptiste Lespiau, L. Sifre, and John M. Jumper. Accelerating large language model decoding with speculative sampling. *ArXiv*, abs/2302.01318, 2023. 2, 3, 5, 8
- [7] Liang Chen, Haozhe Zhao, Tianyu Liu, Shuai Bai, Junyang Lin, Chang Zhou, and Baobao Chang. An image is worth 1/2 tokens after layer 2: Plug-and-play inference acceleration for large vision-language models. In *European Conference on Computer Vision*, 2024. 2, 3, 5, 7, 8, 4
- [8] Tri Dao. Flashattention-2: Faster attention with better parallelism and work partitioning. *ArXiv*, abs/2307.08691, 2023. 3, 8, 4
- [9] DeepSeek-AI, Aixin Liu, Bei Feng, Bing Xue, Bing-Li Wang, Bochao Wu, Chengda Lu, Chenggang Zhao, Chengqi Deng, et al. Deepseek-v3 technical report. *ArXiv*, abs/2412.19437, 2024. 1
- [10] Cunxiao Du, Jing Jiang, Xu Yuanchen, Jiawei Wu, Sicheng Yu, Yongqi Li, Shenggui Li, Kai Xu, Liqiang Nie, Zhaopeng Tu, et al. Glide with a cape: A low-hassle method to accelerate speculative decoding. *arXiv preprint arXiv:2402.02082*, 2024. 8
- [11] Mark Endo, Xiaohan Wang, and Serena Yeung-Levy. Feather the throttle: Revisiting visual token pruning for vision-language model acceleration. *ArXiv*, abs/2412.13180, 2024. 2, 3, 4
- [12] Xinyu Fang, Kangrui Mao, Haodong Duan, Xiangyu Zhao, Yining Li, Dahua Lin, and Kai Chen. Mmbench-video: A long-form multi-shot benchmark for holistic video understanding. *ArXiv*, abs/2406.14515, 2024. 1
- [13] Chaoyou Fu, Yuhan Dai, Yondong Luo, Lei Li, Shuhuai Ren, Renrui Zhang, Zihan Wang, Chenyu Zhou, Yunhang Shen, Mengdan Zhang, Peixian Chen, Yanwei Li, Shaohui Lin, Sirui Zhao, Ke Li, Tong Xu, Xiawu Zheng, Enhong Chen, Rongrong Ji, and Xing Sun. Video-mme: The first-ever comprehensive evaluation benchmark of multi-modal llms in video analysis. *2025 IEEE/CVF Conference on Computer Vision and Pattern Recognition (CVPR)*, pages 24108–24118, 2024. 5, 1
- [14] Yichao Fu, Peter Bailis, Ion Stoica, and Hao Zhang. Break the sequential dependency of llm inference using lookahead decoding. *arXiv preprint arXiv:2402.02057*, 2024. 8
- [15] Mukul Gagrani, Raghav Goel, Wonseok Jeon, Junyoung Park, Mingu Lee, and Christopher Lott. On speculative decoding for multimodal large language models. *ArXiv*, abs/2404.08856, 2024. 5, 8
- [16] Haiduo Huang, Fuwei Yang, Zhenhua Liu, Xuanwu Yin, Dong Li, Pengju Ren, and Emad Barsoum. Specvlm: Fast speculative decoding in vision-language models. 2025. 8
- [17] Xiaohu Huang, Hao Zhou, and Kai Han. Prunevid: Visual token pruning for efficient video large language models. *ArXiv*, abs/2412.16117, 2024. 8
- [18] Yicheng Ji, Jun Zhang, Heming Xia, Jinpeng Chen, Lidan Shou, Gang Chen, and Huan Li. Specvlm: Enhancing speculative decoding of video llms via verifier-guided token pruning. *ArXiv*, abs/2508.16201, 2025. 2, 3, 5, 6, 7, 8
- [19] Yaniv Leviathan, Matan Kalman, and Yossi Matias. Fast inference from transformers via speculative decoding. In *International Conference on Machine Learning*, 2022. 2, 3, 8, 1
- [20] Bo Li, Yuanhan Zhang, Dong Guo, Renrui Zhang, Feng Li, Hao Zhang, Kaichen Zhang, Yanwei Li, Ziwei Liu, and Chunyuan Li. Llava-onevision: Easy visual task transfer. *ArXiv*, abs/2408.03326, 2024. 1, 2, 6
- [21] Kunchang Li, Yali Wang, Yanan He, Yizhuo Li, Yi Wang, Yi Liu, Zun Wang, Jilan Xu, Guo Chen, Ping Luo, Limin Wang, and Yu Qiao. Mvbench: A comprehensive multi-modal video understanding benchmark. *2024 IEEE/CVF Conference on Computer Vision and Pattern Recognition (CVPR)*, pages 22195–22206, 2023. 5, 1
- [22] Yuhui Li, Fangyun Wei, Chao Zhang, and Hongyang Zhang. Eagle-2: Faster inference of language models with dynamic draft trees. In *Conference on Empirical Methods in Natural Language Processing*, 2024. 8
- [23] Yuhui Li, Fangyun Wei, Chao Zhang, and Hongyang Zhang. Eagle: Speculative sampling requires rethinking feature uncertainty. *ArXiv*, abs/2401.15077, 2024. 5, 8, 1, 2
- [24] Yanwei Li, Yuechen Zhang, Chengyao Wang, Zhisheng Zhong, Yixin Chen, Ruihang Chu, Shaoteng Liu, and Jiaya Jia. Mini-gemini: Mining the potential of multi-modality vision language models. *ArXiv*, abs/2403.18814, 2024. 1
- [25] Yuhui Li, Fangyun Wei, Chao Zhang, and Hongyang Zhang. Eagle-3: Scaling up inference acceleration of large language models via training-time test. *ArXiv*, abs/2503.01840, 2025. 8, 1
- [26] Bin Lin, Bin Zhu, Yang Ye, Munan Ning, Peng Jin, and Li Yuan. Video-llava: Learning united visual representation by alignment before projection. *ArXiv*, abs/2311.10122, 2023. 1
- [27] Haotian Liu, Chunyuan Li, Qingyang Wu, and Yong Jae Lee. Visual instruction tuning. *ArXiv*, abs/2304.08485, 2023. 1
- [28] Haitong Liu, Kuofeng Gao, Yang Bai, Jinmin Li, Jinxiao Shan, Tao Dai, and Shu-Tao Xia. Protecting your video

- content: Disrupting automated video-based llm annotations. *2025 IEEE/CVF Conference on Computer Vision and Pattern Recognition (CVPR)*, pages 24056–24065, 2025. 1
- [29] Tianyu Liu, Yun Li, Qitan Lv, Kai Liu, Jianchen Zhu, and Winston Hu. Parallel speculative decoding with adaptive draft length. *ArXiv*, abs/2408.11850, 2024. 5, 6, 8, 1, 2
- [30] Xuyang Liu, Yiyu Wang, Junpeng Ma, and Linfeng Zhang. Video compression commander: Plug-and-play inference acceleration for video large language models. *arXiv preprint arXiv:2505.14454*, 2025. 8
- [31] LMMs-Lab. Video detail caption, 2024. Accessed: 2024-11-5, 1
- [32] Machel Reid, Nikolay Savinov, Denis Teplyashin, Dmitry Lepikhin, Timothy P. Lillicrap, Jean-Baptiste Alayrac, Radu Soricut, Angeliki Lazaridou, Orhan Firat, Julian Schrittwieser, et al. Gemini 1.5: Unlocking multimodal understanding across millions of tokens of context. *ArXiv*, abs/2403.05530, 2024. 1
- [33] Yuzhang Shang, Mu Cai, Bingxin Xu, Yong Jae Lee, and Yan Yan. Llava-prumerge: Adaptive token reduction for efficient large multimodal models. *ArXiv*, abs/2403.15388, 2024. 8
- [34] Hao Shao, Yuxuan Hu, Letian Wang, Steven L. Waslander, Yu Liu, and Hongsheng Li. Lmdrive: Closed-loop end-to-end driving with large language models. *2024 IEEE/CVF Conference on Computer Vision and Pattern Recognition (CVPR)*, pages 15120–15130, 2023. 1
- [35] Zhenwei Shao, Mingyang Wang, Zhou Yu, Wenwen Pan, Yan Yang, Tao Wei, Hongyuan Zhang, Ning Mao, Wei Chen, and Jun Yu. Growing a twig to accelerate large vision-language models. *ArXiv*, abs/2503.14075, 2025. 8
- [36] Leqi Shen, Guoqiang Gong, Tao He, Yifeng Zhang, Pengzhang Liu, Sicheng Zhao, and Guiguang Ding. Fastvid: Dynamic density pruning for fast video large language models. *ArXiv*, abs/2503.11187, 2025. 8
- [37] Yuhao Shen, Junyi Shen, Quan Kong, Tianyu Liu, Yao Lu, and Cong Wang. Speculative decoding via hybrid drafting and rollback-aware branch parallelism. *ArXiv*, abs/2506.01979, 2025. 6, 8, 2, 3
- [38] Xi Tang, Jihao Qiu, Lingxi Xie, Yunjie Tian, Jianbin Jiao, and Qixiang Ye. Adaptive keyframe sampling for long video understanding. *2025 IEEE/CVF Conference on Computer Vision and Pattern Recognition (CVPR)*, pages 29118–29128, 2025. 8
- [39] Keda Tao, Can Qin, Haoxuan You, Yang Sui, and Huan Wang. Dycoke : Dynamic compression of tokens for fast video large language models. *2025 IEEE/CVF Conference on Computer Vision and Pattern Recognition (CVPR)*, pages 18992–19001, 2024. 2, 5, 7, 8, 4
- [40] Hugo Touvron, Thibaut Lavril, Gautier Izacard, Xavier Martinet, Marie-Anne Lachaux, Timothée Lacroix, Baptiste Rozière, Naman Goyal, Eric Hambro, Faisal Azhar, et al. Llama: Open and efficient foundation language models. *ArXiv*, abs/2302.13971, 2023. 1
- [41] Ashish Vaswani, Noam M. Shazeer, Niki Parmar, Jakob Uszkoreit, Llion Jones, Aidan N. Gomez, Lukasz Kaiser, and Illia Polosukhin. Attention is all you need. In *Neural Information Processing Systems*, 2017. 2
- [42] Zichen Wen, Yifeng Gao, Shaobo Wang, Junyuan Zhang, Qintong Zhang, Weijia Li, Conghui He, and Linfeng Zhang. Stop looking for important tokens in multimodal language models: Duplication matters more. *arXiv preprint arXiv:2502.11494*, 2025. 8
- [43] Haoning Wu, Dongxu Li, Bei Chen, and Junnan Li. Longvideobench: A benchmark for long-context interleaved video-language understanding. *ArXiv*, abs/2407.15754, 2024. 5, 1
- [44] Jinyang Wu, Guocheng Zhai, Ruihan Jin, Jiahao Yuan, Yuhao Shen, Shuai Zhang, Zhengqi Wen, and Jianhua Tao. Atlas: Orchestrating heterogeneous models and tools for multi-domain complex reasoning. *arXiv preprint arXiv:2601.03872*, 2026. 1
- [45] Heming Xia, Tao Ge, Peiyi Wang, Si-Qing Chen, Furu Wei, and Zhifang Sui. Speculative decoding: Exploiting speculative execution for accelerating seq2seq generation. In *Conference on Empirical Methods in Natural Language Processing*, 2022. 2, 3, 8, 1
- [46] Guangxuan Xiao, Yuandong Tian, Beidi Chen, Song Han, and Mike Lewis. Efficient streaming language models with attention sinks. *ArXiv*, abs/2309.17453, 2023. 3
- [47] Long Xing, Qidong Huang, Xiao wen Dong, Jiajie Lu, Pan Zhang, Yuhang Zang, Yuhang Cao, Conghui He, Jiaqi Wang, Feng Wu, and Dahua Lin. Pyramidrop: Accelerating your large vision-language models via pyramid visual redundancy reduction. *ArXiv*, abs/2410.17247, 2024. 2, 5, 7, 8, 4
- [48] Senqiao Yang, Yukang Chen, Zhuotao Tian, Chengyao Wang, Jingyao Li, Bei Yu, and Jiaya Jia. Visionzip: Longer is better but not necessary in vision language models. *2025 IEEE/CVF Conference on Computer Vision and Pattern Recognition (CVPR)*, pages 19792–19802, 2024. 8
- [49] Xuan Zhang, Cunxiao Du, Sicheng Yu, Jiawei Wu, Fengzhuo Zhang, Wei Gao, and Qian Liu. Sparse-to-dense: A free lunch for lossless acceleration of video understanding in llms. In *Annual Meeting of the Association for Computational Linguistics*, 2025. 5, 6, 7, 8
- [50] Yuan Zhang, Chunkai Fan, Junpeng Ma, Wenzhao Zheng, Tao Huang, Kuan Cheng, Denis Gudovskiy, Tomoyuki Okuno, Yohei Nakata, Kurt Keutzer, and Shanghang Zhang. Sparsevlm: Visual token sparsification for efficient vision-language model inference. *ArXiv*, abs/2410.04417, 2024. 2, 5, 6, 7, 8, 4
- [51] Weilin Zhao, Yuxiang Huang, Xu Han, Wang Xu, Chaojun Xiao, Xinrong Zhang, Yewei Fang, Kaihuo Zhang, Zhiyuan Liu, and Maosong Sun. Ouroboros: Generating longer drafts phrase by phrase for faster speculative decoding. In *Conference on Empirical Methods in Natural Language Processing*, 2024. 8
- [52] Junjie Zhou, Yan Shu, Bo Zhao, Boya Wu, Shitao Xiao, Xi Yang, Yongping Xiong, Bo Zhang, Tiejun Huang, and Zheng Liu. Mlvu: A comprehensive benchmark for multi-task long video understanding. *ArXiv*, abs/2406.04264, 2024. 5, 1

# ParallelVLM: Lossless Video-LLM Acceleration with Visual Alignment Aware Parallel Speculative Decoding

## Supplementary Material

For readers who are not familiar with speculative decoding and parallel decoding, we provide more detailed explanations in the appendix. The appendix is organized as follows: experimental details are presented in Sec. A, parallel decoding in Sec. B, and theoretical analysis of the proposed method in Sec. C. Additionally, we elaborate on the origin of the unbiased nature of UV-Prune in Sec. D. Finally, we include several illustrative case studies in Sec. E.

### A. Experimental Details

**Tasks and Metrics.** Since speculative decoding [19, 45] focuses on accelerating long-paragraph decoding, we select five video understanding and description datasets VideoDetailCaption [31], VideoMME [13], MVBench [21], MVLU [52], LongVideoBench [43] with rich semantic information. We filter out videos shorter than one minute and randomly sample 50 samples from each dataset for evaluation. Unlike traditional Visual Question Answering (VQA) formats<sup>1</sup>, we employ prompt engineering to generate finer-grained descriptions. For the lossy visual token pruning method, due to the lack of long, detailed ground truth description labels in the community, we save the autoregressive output texts after pruning and use the target model with full context to perform token-wise speculative sampling [19] to measure the acceptance rate  $\mathcal{A}$ . This approach not only saves the cost of manual annotation, but also accurately reflects the distribution shifts of the pruned models.

**Model Combinations.** Regarding the model combinations, since ParallelVLM is a training-free method, aligning the draft model with the target model poses a challenge. We therefore select model combinations with different parameter sizes from the same series to ensure that the draft and target models have a basic alignment capability. In experiments we find that models from the LLaVA-OV [20] series exhibit a higher alignment ( $M = 8.31$  for 0.5B/7B and  $M = 6.83$  for 7B/72B), while Qwen2.5-VL [3] shows a relatively lower alignment ( $M = 4.28$  for 7B/32B). Additionally, the 0.5B/7B combination within the LLaVA-OV series achieves better alignment than the 7B/72B combination, as the former has more similar model capacities and fine-tuning data scales. Although our approach is totally training-free, draft training-based methods [5, 23, 25] can be seamlessly integrated to achieve improved alignment and higher acceleration ratios in future work.

<sup>1</sup>Different from our finer-grained long-paragraph decoding setting, VQA evaluation suites like LLMs-Eval mainly focus on reality checking.

Table 5. Sensitivity of speed ratio  $c = T_p/T_q$  with the increase of pruning ratio  $\alpha$ . The forward time is reported in ms.

Models	Target $T_p$	Draft $T_q$		
		$\alpha = 0.0$	$\alpha = 0.5$	$\alpha = 0.9$
LLaVA-OV (0.5B & 7B)	78.3 ( $\pm 3.46$ )	46.1 ( $\pm 1.21$ ) $c = 1.7$	32.5 ( $\pm 0.89$ ) $c = 2.4$	25.8 ( $\pm 0.32$ ) $c = 3.0$
LLaVA-OV (7B & 72B)	420 ( $\pm 8.64$ )	78.3 ( $\pm 3.46$ ) $c = 5.3$	57.5 ( $\pm 2.38$ ) $c = 7.3$	46.6 ( $\pm 1.52$ ) $c = 9.0$
Qwen2.5-VL (7B & 32B)	203 ( $\pm 6.89$ )	63.7 ( $\pm 2.42$ ) $c = 3.2$	48.2 ( $\pm 1.66$ ) $c = 4.2$	39.8 ( $\pm 1.24$ ) $c = 5.1$
LLaVA-OV (7B & 7B)	78.3 ( $\pm 3.46$ )	78.3 ( $\pm 3.46$ ) $c = 1.0$	57.5 ( $\pm 2.38$ ) $c = 1.4$	46.6 ( $\pm 1.52$ ) $c = 1.7$
Qwen2.5-VL (7B & 7B)	63.7 ( $\pm 2.42$ )	63.7 ( $\pm 2.42$ ) $c = 1.0$	48.2 ( $\pm 1.66$ ) $c = 1.3$	39.8 ( $\pm 1.24$ ) $c = 1.6$

Table 6. Peak memory usage (GB) and latency breakdown of LLaVA-OV-7B/72B (s). The output length is set to 512.

Operation	Method		
	Autoregressive	SD	ParallelVLM
Peak Memory	198.85	225.19	225.34
Draft Prefill	7.92	7.92	/
Target Prefill	44.23	44.23	44.23
Draft Decode	/	58.14	/
Target Decode	228.14	54.85	67.85
Token/s	2.25	4.53	7.55
Total Latency	280.29	165.15	112.08

**Window Size  $\gamma$  Selection.** For simplicity of explanation in the main text, we directly rounded the speed ratio between the draft model and the target model  $c = T_p/T_q$  to an integer value. In practice, their acceleration ratio is not strictly an integer. In Tab. 5, we present the exact acceleration ratios for all the five combinations. Rounding the window size up or down relative to the speed ratio  $c$  are both reasonable options, the superiority between which depends on the relative magnitudes of the window size  $\gamma$  and the mean accepted length  $M$  [29]. For combinations of LLaVA-OV-7B/72B and Qwen2.5-VL-7B/32B with aggressive window sizes and relatively conservative accepted lengths, rounding down to reduce mutual waiting is a wiser choice. For Self-SD with narrow window sizes and high accepted lengths, rounding up is a more sensible option.

**Memory Consumption and Latency Breakdown.** We report the peak memory usage and latency breakdown in Tab. 6. Although performing the draft/target forward func-

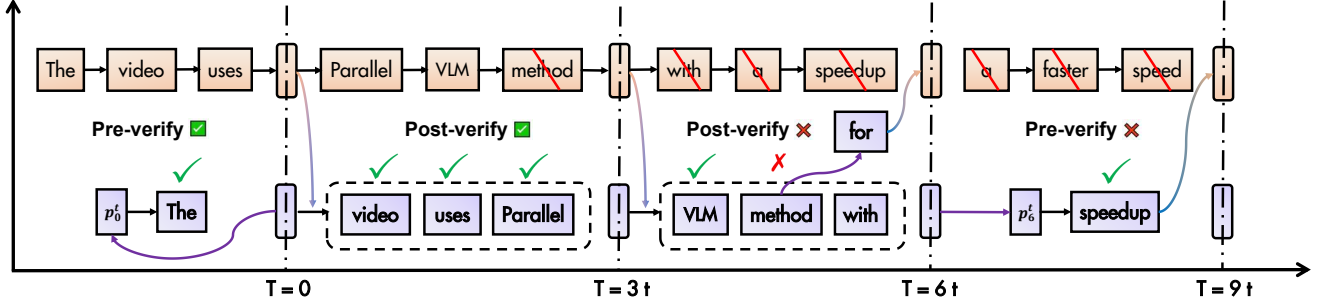


Figure 8. An illustrative example of decoding “The video uses ParallelVLM for speedup” is provided to demonstrate the verification mode switching of the parallel pipeline, as well as its advancement and rollback mechanisms. Here  $t$  denotes the one single forward time of the draft model and the window size  $\gamma$  is set to 3.

tions simultaneously, ParallelVLM incurs no more memory footprint beyond vanilla SD with draft model pruning (+26 GB than autoregressive). Furthermore, ParallelVLM directly saves the draft model’s prefilling time with parallel prefilling (−7.92 s), and significantly accelerates the decoding speed through the visual alignment aware parallelism. Our approach achieves a notable 7.55 tokens/s throughput, which is  $3.36\times$  faster than autoregressive decoding. While the throughput metric may vary on different devices, the speedup ratio will persist for methodological superiority.

**Tree-Attention Integration.** Applying a draft tree structure to speculative decoding can help improve the accepted length, but it is not feasible under a parallel architecture. The draft tree generates KV caches for multiple candidates, which constitutes a batch of additional overhead. This overhead grows exponentially with the depth  $h$  of the tree during parallelization (even sparse trees [23] exhibit considerable growth). In vanilla speculative decoding, the depth of the draft tree is generally equal to the window size  $h = \gamma$ . However, for parallel decoding, the depth of the draft tree depends on the adaptive draft length [29] and may increase  $h$  by multiple times. To address the limitation of applying the tree structure to parallel decoding, SpecBranch [37] attempts to achieve a balance with a sparser “branch prediction” structure, which we anticipate will find broader applications in the future.

## B. Parallel Pipeline Details

For clarity, we collectively denote the prefix of visual-text tokens  $V_{1:m}, X_{1:n}$  as  $\mathbf{x}$  here to describe the pipeline advancement and rollback mechanisms of parallel decoding.

As illustrated in Algorithm. 1, Parallel SD [29] sets two verification modes for the target model: (i) Pre-verify, which verifies the first draft token in advance, and (ii) Post-verify, which performs batch verification meanwhile generating new draft tokens. We elaborate on more details in the following with the illustrative example in Fig. 8 of decoding the sentence “The video uses ParallelVLM for speedup” with the window size  $\gamma = 3$ .

---

### Algorithm 1 Parallel Decoding Pipeline.

---

**Require:** draft model  $M_q$ , target model  $M_p$ , input prefix  $\mathbf{x}$ , output length  $K$ , window size  $\gamma$ .

- 1: mode  $\leftarrow$  “Pre-verify”
  - 2: **while**  $\text{len}(\mathbf{x}) < K$  **do**
  - 3:   **if** mode = “Pre-verify” **then**
  - 4:      $(\mathbf{x}, \text{mode}) \leftarrow \text{Pre-verify}(M_q, M_p, \mathbf{x}, \gamma)$
  - 5:   **else**
  - 6:      $(\mathbf{x}, \text{mode}) \leftarrow \text{Post-verify}(M_q, M_p, \mathbf{x}, \gamma)$
  - 7:   **end if**
  - 8: **end while**
- 

At  $T = 0$ , both the draft model and the target model complete pre-filling, they output a bonus token and execute the initial Pre-verify. The Pre-verify verifies the first token “The” before the verification stage. Upon successful matching (accept “The”), the mode switches to Post-verify. From  $T = 0 \sim 3t$ , a window size of draft tokens “video uses Parallel” is waiting to be verified. The Post-verify checks them with batch parallelism, accepts them all, and maintains the Post-verify mode. From  $T = 3t \sim 6t$ , another window size of draft tokens “VLM method with” is waiting to be verified. However, “method” is rejected by the target model, so a new token “for” is resampled from the target’s distribution. The KV cache of the draft model rollbacks to “VLM” and starts from “for” to draft new tokens, meanwhile the mode is reset back to Pre-verify. From  $T = 6t \sim 9t$ , since there are no draft tokens left, the target model verifies the first draft token “a”. Unfortunately, the target model rejects it and thinks that the resampled “speedup” is a better choice. The KV cache of the draft model thus rollbacks to “for” and restarts from “speedup” to continue its drafting. The whole pipeline from  $T = 0 \sim 9t$  thus outputs “The video uses ParallelVLM for speedup” within only three target model verification times. The maximum adaptive draft length [29] here is 5, as “The video uses ParallelVLM” is continuous without interruption of the first two draft stages.

## C. Theoretical Analysis

Let  $T_q = t$  be the single forward time of the draft model and  $T_p = c \cdot t$  be the verification time of the target model. For a predefined hyperparameter  $\gamma$  to control window size, we derive the ideal and practical speedup ratio by calculating the per-token time, respectively.

**Theorem 2** (Vanilla SD (Ideal)). *Under full acceptance of the  $\gamma$  draft tokens, the per-token time of vanilla SD is:*

$$T_{SD} = \frac{\gamma \cdot T_q + T_p}{\gamma + 1} = \frac{\gamma + c}{\gamma + 1} \cdot t. \quad (8)$$

Thus, the ideal speedup ratio is  $\mathcal{V}_{SD} = \frac{T_p}{T_{SD}} = c \cdot \frac{\gamma + 1}{\gamma + c}$ .

**Theorem 3** (Parallel SD (Ideal)). *Under full acceptance of the  $\gamma$  draft tokens, the per-token time of parallel SD is:*

$$T_{PSD} = \frac{\max(\gamma t, ct)}{\gamma} = \begin{cases} t, & \gamma \geq c \\ \frac{c}{\gamma} t, & \gamma < c \end{cases} \quad (9)$$

When  $\gamma = c$ , the ideal speedup ratio is  $\mathcal{V}_{PSD} = \frac{T_p}{T_{PSD}} = c$ , representing  $c \times$  speedup versus autoregressive decoding and  $\mathcal{V}_{PSD}/\mathcal{V}_{SD} = \frac{\gamma + c}{\gamma + 1} = \frac{2c}{c + 1} \rightarrow 2 \times (c \gg 1)$  speedup compared to vanilla SD. Note that  $\mathcal{V}_{PSD}$  can enjoy a higher gain of  $c^* > c$  with our draft model pruning setting.

**Theorem 4** (Vanilla SD (Practical)). *Under partial acceptance rate  $\tau$  ( $0 < \tau < 1$ ) of  $\gamma$  draft tokens, the per-token time of vanilla SD is:*

$$T_{SD} = \frac{\gamma \cdot T_q + T_p}{\tau \cdot \gamma + 1} = \frac{\gamma + c}{\tau \cdot \gamma + 1} \cdot t. \quad (10)$$

Thus, the ideal speedup ratio is  $\mathcal{V}_{SD} = \frac{T_p}{T_{SD}} = c \cdot \frac{\tau \cdot \gamma + 1}{\gamma + c}$ , which increases monotonically with the acceptance rate  $\tau$ .

**Theorem 5** (Parallel SD (Practical)). *Under partial acceptance rate  $\tau$  ( $0 < \tau < 1$ ) of  $\gamma$  draft tokens, the per-token time of parallel SD is:*

$$T_{PSD} = \frac{\max(\gamma t, ct)}{\tau \cdot \gamma} = \begin{cases} \frac{1}{\tau} t, & \gamma \geq c \\ \frac{c}{\tau \cdot \gamma} t, & \gamma < c \end{cases} \quad (11)$$

When  $\gamma = c$ , the practical speedup ratio is  $\mathcal{V}_{PSD} = \frac{T_p}{T_{PSD}} = \tau \cdot c$ , which also increases monotonically with the acceptance rate  $\tau$ . Recall that Theorem. 1 gives  $\mathcal{V}_{iPSD} = \hat{\tau}(\mathcal{P}, \alpha) \cdot c^*(\alpha)$ . It represents an expanded speed ratio  $c^*(\alpha) > c$  with a robust acceptance rate  $\hat{\tau}(\mathcal{P}, \alpha)$ , where  $\mathcal{P}$  is the visual alignment aware pruning and  $\alpha$  is the pruning ratio.  $\mathcal{V}_{iPSD}$  strikes a balance between  $c^*(\alpha)$  and  $\hat{\tau}(\mathcal{P}, \alpha)$  that exceeds  $\mathcal{V}_{PSD}$  by up to  $0.3 \sim 0.4 \times$  (see Fig. 6 (a)).

Although Theorem. 2 - 5 provide general illustrations, the theoretical speedup ratio of parallel decoding is actually more complex in practice. As described in Sec. B, the

above theory holds only in Post-verify mode; however, if pre-verify (resulting from rollbacks) is taken into account, analysis must be conducted based on the distribution of accepted lengths. Following SpecBranch [37], we assume the random variable of the accepted lengths  $X$  follows a truncated geometric distribution  $X \sim TruncGeo(\tau, \gamma)$ .

**Lemma 1** (Expected Draft Accepted Length). For truncated geometric distribution  $X \sim TruncGeo(\tau, \gamma)$ ,

$$E[X] = \frac{\tau(1 - \tau^\gamma)}{1 - \tau}. \quad (12)$$

*Proof.* Expand the expected value of random variable  $X$ ,

$$\begin{aligned} E[X] &= \sum_{k=0}^{\gamma} k \cdot \mathbb{P}(X = k) \\ &= \sum_{k=0}^{\gamma-1} k \cdot (1 - \tau)\tau^k + \gamma \cdot \tau^\gamma. \end{aligned}$$

Let  $S = \sum_{k=0}^{\gamma-1} \tau^k = \frac{1 - \tau^\gamma}{1 - \tau}$ . Take differentiation regarding  $\tau$ , we have,

$$\frac{dS}{d\tau} = \sum_{k=0}^{\gamma-1} k\tau^{k-1} = \frac{1 - \gamma\tau^{\gamma-1} + (\gamma - 1)\tau^\gamma}{(1 - \tau)^2}$$

$$E[X] = (1 - \tau)\tau \cdot \frac{dS}{d\tau} + \gamma \cdot \tau^\gamma = \frac{\tau(1 - \tau^\gamma)}{1 - \tau} \quad \square$$

**Theorem 6** (Parallel SD (with Rollback)). *The per-token time of parallel SD under rollback is,*

$$T_{PSD_r} = \frac{2 \cdot \max(\gamma t, ct)}{(1 + \tau\gamma) \cdot \frac{\tau(1 - \tau^\gamma)}{1 - \tau}}. \quad (13)$$

*Proof.* Define the acceptance vector  $\omega = (\omega_1, \dots, \omega_\gamma) \in \{0, 1\}^\gamma$ , where  $\omega_i = 1$  if and only if token  $i$  is accepted. The accepted token count is,

$$X = \sum_{i=1}^{\gamma} \omega_i, \quad \mathbb{P}(\omega_i = 1) = \tau \text{ (i.i.d.)}.$$

To compute the total number of tokens with retry, define two round of: 1)  $\gamma$  tokens (accepted if  $\omega = 1$ ); 2) Retry if Round 1 fails, which yields  $E[X]$  tokens. Thus, the total expectation is:

$$\begin{aligned} E_{total} &= \tau^\gamma(\gamma + E[X]) + (1 - \tau^\gamma) \frac{(E[X] - \gamma\tau^\gamma)}{1 - \tau^\gamma} \\ &= (1 + \tau^\gamma) \cdot E[X] \end{aligned}$$

This implies that Parallel SD (with Rollback) achieves an acceleration of  $(1 + \tau^\gamma) \times$  compared to vanilla SD (with

Rollback). As  $\tau \rightarrow 1$ , the acceleration ratio reaches  $2\times$ , matching the ideal case in Theorem. 3. Thus, we calculate the per-token time with the two rounds:

$$T_{PSD_r} = \frac{T_{total}}{E_{total}} = \frac{2 \cdot \max(\gamma t, ct)}{(1 + \tau^\gamma) \cdot \frac{\tau(1-\tau^\gamma)}{1-\tau}}. \quad \square$$

When  $\gamma = c$ , the speedup ratio of Parallel SD with rollback is  $\mathcal{V}_{PSD_r} = \frac{T_p}{T_{PSD_r}} = \frac{1}{2} \sum_{k=1}^{2c} \tau^k$ . It increases monotonically with the acceptance rate  $\tau$  in polynomial order, so maintaining robust acceptance rates is even more crucial for parallel decoding. ParallelVLM increases  $c$  by pruning and keeps an unbiased alignment for higher  $\tau$ , achieving considerable speedup. As shown in Tab. 7, under the extreme pruning ratio  $\alpha \rightarrow 1$  where  $c^*(\alpha)$  keeps almost the same, we observe the rapid decrease of speedup ratio with lower acceptance rates, confirming the high-sensitivity effect of parallel decoding performance on acceptance rates and the necessity of the visual alignment aware pruning.

Table 7. Experiments with LLaVA-OV-7B/72B on VideoDetail-Caption under extremely higher pruning ratio ( $\alpha \rightarrow 1$ ).

Pruning ratio $\alpha$	0.90	0.95	0.99	1.00
Accepted Lengths $M$	6.82	6.53	5.74	4.53
Acceptance rates $\tau$	0.41	0.37	0.33	0.27
Speedup	$3.43\times$	$3.28\times$	$2.90\times$	$2.53\times$

## D. Why is UV-Prune Essential?

In recent years, numerous studies have focused on pruning VLMs [7, 39, 47, 50] to achieve inference acceleration at the cost of a certain degree of generation quality. In contrast, our work explores the transfer of video-based understanding from more powerful target models to draft models, making it orthogonal to prior research. We retain the full context of the target model to ensure theoretically lossless generation, and perform pruning on the draft model to align with the target model – marking the first application in parallel decoding framework to allow window size expansion.

Feather [11] has discussed the issue of positional bias in the image domain. They observe that the shallow layers of LLMs serve as “active” regions for visual token comprehension and attribute the attention bias at the vision-text boundaries to the more similar RoPE positional encodings. By computing attention scores without positional encodings as the criterion, they achieve better performance gains.

However, directly applying Feather’s method is no longer feasible for the target model to guide the draft model pruning. The target and draft models differ greatly in embedding dimensions and network depth, leading to architectural mismatch when performing intra-LLM pruning directly on the draft model. In addition, Feather [11] requires

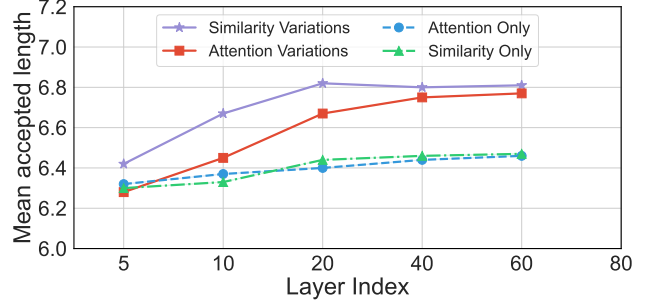


Figure 9. Experiments with LLaVA-OV-7B/72B on VideoDetail-Caption with different draft model pruning strategies.

re-computation of the target model’s attention scores without RoPE, which is not only time-consuming but also conflicts with FlashAttention [8].

To avoid introducing additional computations and ensure compatibility with FlashAttention, we adopt token representations from the shallow layers of the target model as the pruning anchors. Since attention itself is a similarity weight, using cross-modal (vision-text) similarity is a well-motivated approach. To further eliminate the bias induced by positional encodings, we calculate the similarity variations of visual tokens at each position layer by layer to “offset” the interference of positional encodings. In this way, UV-Prune accurately identifies the few key video tokens prioritized by the target model among a large number of tokens, and effectively transfers this focus to the draft model, achieving salient yet robust image-text relevance.

As shown in Fig. 9, both variation and similarity enhance the effectiveness of video token selection. The variation mechanism of UV-Prune mitigates “positional bias”, leading to significant improvements for both attention and similarity criterion. We also observe that similarity-variation converges at  $L = 20$  (and it generalizes well for different model combinations). Thus, we predefine  $L = 20$  as the number of layers for the target model to guide the draft model’s pruning. The propagation of token representations in such shallow layers consumes negligible transmission time ( $\sim 0.01$  s) and ensures that the subsequent pre-filling of the draft model is fully hidden within the target model’s pre-filling span. Most importantly, our alignment-aware pruning method meets the requirement for robust acceptance rates specified in Theorem 6.

## E. Case Study

We present two generation paragraphs in Fig. 10 (LLaVA-7B/72B) and Fig. 11 (Qwen2.5-VL-7B/32B) to intuitively demonstrate the effects of unbiased pruning guided by the target model in long-sequence video tokens, as well as the lossless generation performance of ParallelVLM compared to lossy visual token pruning schemes. We observe that ParallelVLM maintains finer-grained details and accurately reflects the realities in the videos.

### LLaVA-OV-7B-72B



Please provide a detailed description of the video, focusing on the main subjects, their actions and the background scenes.



**FastV:** The video opens with a news studio scene where two anchors are seated at a desk with a backdrop displaying the news channel's logo and the words 'Health News.' The scene transitions to a live report on snowy conditions, with a reporter standing outdoors in front of a snow-covered street. The reporter is dressed in a black jacket and is speaking to the camera. The scene then shows a woman in a blue shirt and jeans shoveling snow from a driveway. The video continues with the reporter interviewing a woman who is also shoveling snow. The woman is wearing a black coat and a scarf, and she is holding a yellow shovel. The background shows parked cars ...

**ParallelVLM:** The video begins with a news segment titled 'Health News' featuring two anchors in a studio. The background includes a large screen displaying the 'Health News' logo and a heart symbol. The scene transitions to a live report from a snowy outdoor location, where a reporter in a black jacket with a white scarf is seen speaking to the camera. The reporter is standing in front of a snow-covered street with parked cars and a building in the background. The text 'NEWS8 Shoveling Safety' and 'February Freeze' appears on the screen, indicating the topic of the report. A woman is seen shoveling snow with a yellow shovel, clearing a path ...

Figure 10. Case study for LLaVA-OV-7B/72B.

### Qwen2.5-VL-7B-32B



Please provide a detailed description of the video, focusing on the main subjects, their actions and the background scenes.



**FastV:** The video features a lively outdoor dance class, likely part of a public event or festival, given the large crowd and festive atmosphere. Here's a detailed breakdown of the video: ### \*\*Main Subjects:\*\* 1. \*\*Instructor:\*\* - The central figure is a male instructor wearing a white T-shirt with a green logo and black athletic pants. He is leading the dance class, demonstrating energetic dance moves... 2. \*\*Participants:\*\* - A diverse group of people, men and women, are following the instructor's lead. They are dressed in casual, comfortable clothing suitable for exercise, such as tank tops, leggings, and athletic shoes ...

**ParallelVLM:** The video is vibrant and dynamic that combines elements of dance, fitness, and visual artistry. ### \*\*Segment 1: Neon Light Show\*\* The video begins with a mesmerizing display of neon lights ... ### \*\*Segment 2: Outdoor Dance Class\*\* The scene shifts to an outdoor dance class taking place in a large, open area, likely a public square or park. \*\*Instructor:\*\* A male instructor, wearing a white t-shirt and black pants, leads the class. He demonstrates dance moves and exercises, guiding the participants through synchronized routines. \*\*Participants:\*\* A large group of people, mostly women, are participating in ...

Figure 11. Case study for Qwen2.5-VL-7B/32B.